Evaluation of trapping efficiency of optical tweezers by dielectrophoresis

Eirini Papagiakoumou
National Technical University of Athens
Zografou Campus
School of Applied Mathematical and Physical Sciences
Physics Department
15780 Athens, Greece
E-mail: papageir@mail.ntua.gr

Dorel Pietreanu
Carol Davila Medical University
Biophysics Research Group
Bucharest, Romania

Mersini I. Makropoulou
National Technical University of Athens
Zografou Campus
School of Applied Mathematical and Physical Sciences
Physics Department
15780 Athens, Greece

Eugenia Kovacs
Carol Davila Medical University
Biophysics Research Group
Bucharest, Romania

Alexander A. Serafetinides
National Technical University of Athens
Zografou Campus
School of Applied Mathematical and Physical Sciences
Physics Department
15780 Athens, Greece

Abstract. A relatively new method for measuring optically induced forces on microparticles and cells, different from the conventional Brownian motion and viscous drag force calibration methods widely used, is introduced. It makes use of the phenomenon of dielectrophoresis for the calibration of optical tweezers through the dielectrophoretic force calculations. A pair of microelectrodes is fabricated by photolithography on a microscope slide and it is connected to a high-frequency generator. The calibration of the optical tweezers setup is performed by the manipulation of polystyrene beads and yeast cells. Calibration diagrams of the transverse forces versus power are deduced for different cell radii and numerical apertures of the objective lenses. The optical system and the related technique provide a fast and easy method for optical tweezers calibration. [DOI: 10.1117/1.2165176]

Keywords: optical tweezers; force calibration; dielectrophoresis.

Paper 05067RR received Mar. 16, 2005; revised manuscript received Sep. 21, 2005; accepted for publication Sep. 30, 2005; published online Jan. 31, 2006.

1 Introduction

"Optical tweezers" is the common term used during the last two decades to describe the optical force generation and confinement of microscopic particles by a highly focused laser beam, as was first demonstrated by Ashkin et al.[1,2] An optical trap, apart from its use as a particle manipulator, when calibrated can be used to measure the forces exerted on trapped objects as a result of various molecular motors within the cell.[3–5] Other important biological applications are the trapping of cells, bacteria and viruses,[6] manipulation of DNA molecules[7–9] and erythrocytes,[9–12] cell sorting,[13] cell fusion,[14,15] intracellular surgery,[16,17] and neuronal growth in studying how neural circuits are formed.[18] Finally, in biotechnology, the "laser-guided direct writing" technique is used to deposit particles of 100 nm to 10 μm onto solid surfaces.[19,20]

For most of the preceding applications, an exact knowledge of the optical forces applied to the trapped particle is useful and different methods exist for force calibration. Two of them that are widely used are the Brownian motion calibration and the viscous drag force calibration. In the first method, the power spectrum of the position of an isolated particle in an optical trap that experiences random forces due to thermal fluctuations is studied,[21–23] while the second method examines the relative motion of a trapped particle with respect to the surrounding liquid.[24,25] Although there has been more than a decade of intense activity, the agreement between theory and experimental force determination is not usually fully satisfactory,[15] and only in a few cases a good agreement has been found.[26] Theoretical estimations of the trapping forces exist only for a spherical geometry of the trapped particle in two limited size regimes. The geometric optics model is in good agreement with measured forces if the diameter of the trapped object is well above the wavelength of the laser light,[27] whereas the electromagnetic theory approach must be used for particles that are small compared with the wavelength (Rayleigh approximation). In the intermediate regime, where the particle sizes are of the order of the wavelength of the trapping laser, the electromagnetic theory seems

Address all correspondence to Eirini Papagiakoumou, Physics, National Technical University of Athens, 15780 Zografou Campus, Athens, Zografou 15780 Greece. Tel: 00302107722987. Fax: 00302107722928. E-mail: papageir@mail.ntus.gr

1083-3668/2006/11(1)/014035/8/$22.00 © 2006 SPIE

to yield better results than the geometric optics,[28] but there remain discrepancies between theory and experiment for the trapping forces in this regime.

In this paper, we describe a different calibration method for an optical trapping system. The method uses the dielectrophoresis, combined with optical trapping, to determine the relation between the output laser power and the corresponding exerted force. Dielectrophoresis is the term used to describe the polarization and associated motion induced in dielectric particles by a nonuniform electric field. The nonuniformity of the electric field induces a dipole moment, due to the convergence of the field lines. Analytical expressions for the dielectrophoretic force, which depends on the geometry of the used system, can be derived and thus the optical force (which is counterbalanced by the dielectrophoretic one) can also be calculated, in a fast and easy way. Additionally, the study of the dimensionless trapping efficiency is performed by changing the cell diameter and the numerical aperture of the objective lenses.

2 Dielectrophoretic Forces

The term "dielectrophoresis" was first introduced by Pohl in 1958 to describe the forces induced by a nonuniform electric field on a small polarizable but uncharged particle.[29,30] Time-periodic inhomogeneous electric fields induce polarization and subsequent movement of dielectric particles. For a spherical particle of radius r, suspended in a medium of electrical permittivity ε_m, the dipole moment $\mathbf{m}$ arising from the boundary charges is given from the equation:

$$\mathbf{m}(\mathbf{r},\omega) = 4\pi\varepsilon_m r^3 f_{\mathrm{CM}}\mathbf{E}(\mathbf{r}), \tag{1}$$

where $\mathbf{E}(\mathbf{r})$ is the electric field, and f_{CM} is the Clausius-Mossotti factor that includes the electrical properties of the particle and the surrounding medium as well as the frequency f of the ac field. The result is an imbalance in force on the particle, enabling it to migrate usually toward the region of greatest field intensity, e.g., an electrode.[31] The dielectrophoretic force that is induced to a particle $\mathbf{F}$ is given by the following expression:

$$\mathbf{F} = 2\pi r^3 \varepsilon_m \,\mathrm{Re}(f_{\mathrm{CM}})\,\nabla E^2. \tag{2}$$

As we can notice, the force is zero except in areas where the field is nonuniform and is analogous to the volume of the particle as well as the real part of f_{CM}. The electric field is calculated for the actual electrode arrangement. If the sample in the chamber is dielectrically homogeneous, we get a time-independent Laplace equation for the potential of the electric field $\mathbf{E}=-\nabla\phi$. For the spherical particle model, the Clausius-Mossotti factor f_{CM} is given by the equation

$$f_{\mathrm{CM}} = \frac{\varepsilon_p^* - \varepsilon_m^*}{\varepsilon_p^* - 2\varepsilon_m^*}, \tag{3}$$

where ε_p^* and ε_m^* are the complex permittivity of the particle and medium, respectively. The complex permittivity is defined by

$$\varepsilon^* = \varepsilon - j\frac{\sigma}{\omega}, \tag{4}$$

where ε and σ are the dielectric constant and conductivity, respectively, and ω is the angular frequency of the electric field. In Eq. (2), all the quantities are positive except of the real part of f_{CM}, which can take both positive and negative values. This term may vary between -0.5 and $+1$, as a result of the electrical properties of the particle and the medium and the applied frequency. If the factor is positive, then the force exerted on the particle is correspondingly positive and the particle will move toward regions of high electric field gradient (which is the edge of the electrodes in most cases—positive dielectrophoresis, pDEP). Otherwise the force exerted will be negative, and the particle will move toward regions of low electric field gradient (which for example is the area in the middle of the two electrodes—negative dielectrophoresis, nDEP).

3 Materials and Methods

The optical trapping setup is schematically shown in Fig. 1. We used an Ar^+ laser emitting at $\lambda=488$ nm, with a nearly Gaussian 2-mm-diam beam. The laser beam was guided through a lens, with a focal length $f=100$ mm. The lens was placed at the required distance allowing the beam to overfill the objective of a modified commercial microscope (Motic, B1 series), as overfilling of the objective is a very crucial parameter to achieve high trapping efficiency. The laser beam was tightly focused to a spot using either a 40× long-distance working or a 100× immersed oil objective lens, with numerical apertures of 0.65 or 1.30, respectively. The particles were observed through the same optical port that the beam enters the microscope objective, and thus it was necessary to insert a dichroic mirror between the eyepiece and the objective to inject the laser beam. The laser power that was entering the objective varied from 5 to 35 mW, with the objective loss being 10% loss in power. The sample image was observed through the same focusing objective with a CCD video camera on a personal computer and recorded for further analysis. A filter was placed between the eyepiece and the CCD camera to prevent the CCD array from damage. The particles we used for trapping were either yeast cells of diameters from 3.5 to 7.0 μm, washed and diluted in distilled water, or 8-μm-diam polystyrene beads (Fluka Chemie), also diluted in distilled water. The diameter of the cells was measured with an error 5%, while that of the beads were known with an accuracy of about 1%. The particle diameters used in every case were in the range from 3.5 to 8 μm, which is larger than the laser wavelength used ($\sim$0.5 μm), so we are closer to the geometrical optics regime.

The dielectrophoretic chamber consisted of two thin-film electrodes, of thickness $\sim$6000 A, placed at a distance of 100 μm, fabricated using conventional microfabrication processes (photolithography) on the top of a microscope slide (Fig. 2). This configuration was chosen as it is easy to construct and also facilitates the theoretical extraction and numerical calculation of the produced potential and electric field. Note that special care was taken to ensure the maximum possible electrodes uniformity and photolithographic quality, as established through optical examination microscopy of

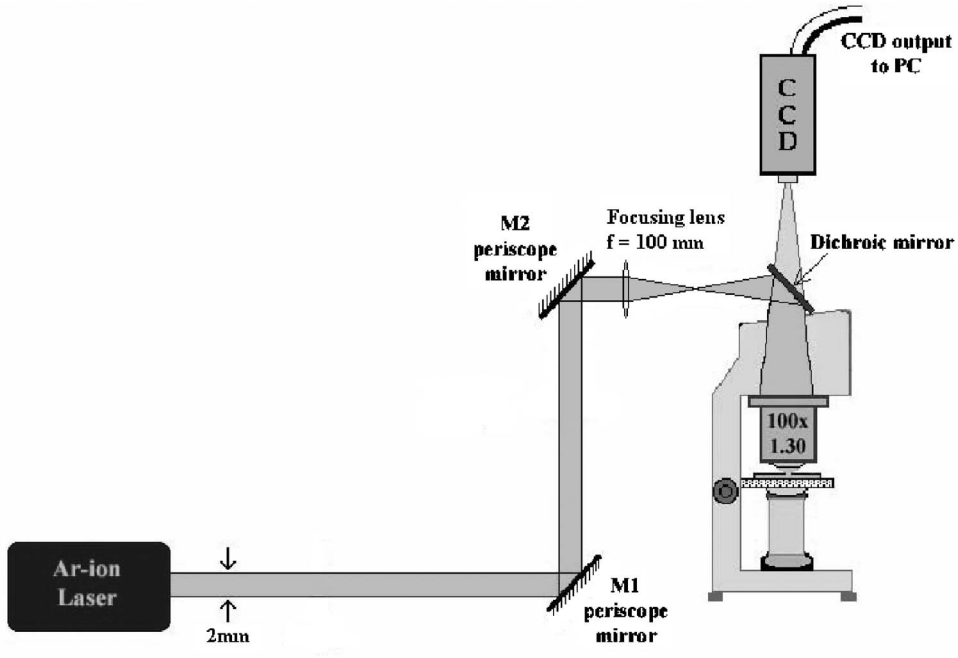

Fig. 1 Experimental setup for optical tweezers based on an Ar^+ laser, emitting at $\lambda = 488$ nm.

100× magnification. To this aim, the best set of electrodes between the several constructed was chosen to be employed in the experimental setup. A quality inspection picture of the electrodes is shown as an insert in Fig. 2. In most cases, the nonuniformity did not exceed 1/10 of the particle size. Despite the preceding, care was taken to trap the particles and repeat the measurements in the most uniform areas of the electrode spacing. Sine wave excitation of 1 MHz and 12 V was applied from a signal generator. Time-periodic inhomogeneous electric fields induce polarization and subsequent movement of the dielectric particles. Frequencies above 50 kHz ensure that distortions of the electrical double layer, induced at the boundary between the particle and the surrounding medium by the electric field, become negligible. The excitation at 1 MHz was selected as it is quite far from 50 kHz and additionally, as shown in Fig. 3, in this area any possible frequency fluctuations do not affect the real part of the Clausius-Mossotti factor $\mathrm{Re}(f_{\mathrm{CM}})$, which is the frequency-dependent parameter of the dielectrophoretic force. In addition, the 1-MHz frequency enables force measurements to be obtained at moderate voltages.

The resulting force on a spherical particle suspended in the medium, due to the dipole moment arising from the boundary charges, enables the particle to move toward regions of high- or low-field intensity, depending on the kind of dielectrophoresis we have. The dielectrophoretic force depends on the intensity of the electric field and the volume of the particle. In our setup, with the easy-to-fabricate 100-μm gap between the two electrodes a voltage of maximum 10 V was required to move the particle.

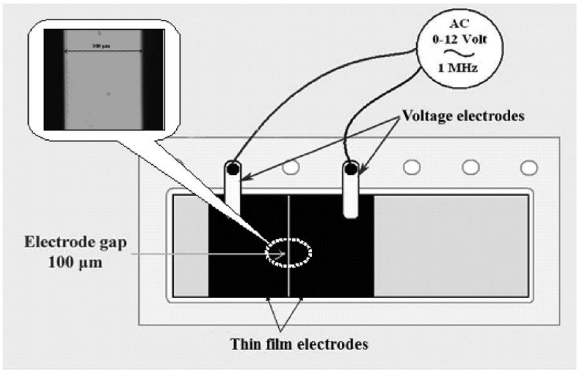

Fig. 2 Schematic presentation of the dielectrophoretic chamber setup and quality inspection picture of the electrodes through optical microscopy examination of 40× magnification.

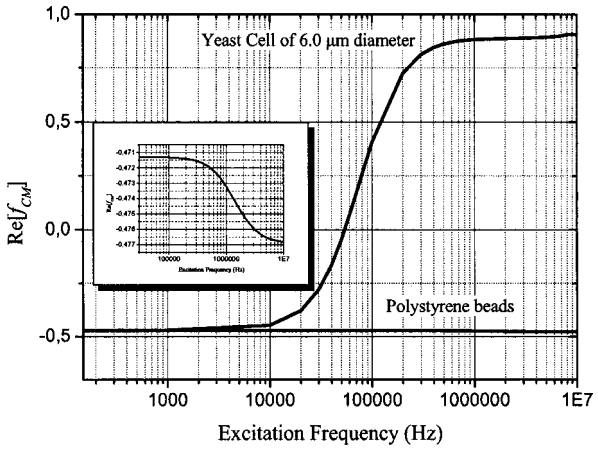

Fig. 3 Frequency dependence of the real part of the Clausius-Mossotti factor for a 6.0-μm-diam yeast cell and for a polystyrene bead. In the inset, we can see the dependence for the case of the polystyrene bead in detail.

To measure the optical trapping force, we used optical tweezers to trap the particle in the space between the two thin electrodes, when no voltage was applied. Then, by increasing the voltage, the particle experienced a dielectrophoretic force, which could be calculated from the determined electric field. The determination of the field between the two planar electrodes was made by using analytical methods based on Green's theorem.[32] Considering the boundary conditions of the electrodynamic problem, which describes our electrode configuration, we derived an expression for the electric potential and from that for the root mean square (rms) of the electric field:[33]

$$E_{\mathrm{rms}}^2 = \frac{V^2}{8\pi^2\Delta^2}\left\{\frac{-8x^2z\Delta + [x^4 + 2x^2(z^2-\Delta^2) + (z^2+\Delta^2)^2]\arctan(2z\Delta/x^2+z^2-\Delta^2)}{[(x-\Delta)^2+z^2][(x+\Delta)^2+z^2]}\right\}^2 + \frac{V^2}{8\pi^2\Delta^2}\left[\frac{4x\Delta(x^2-z^2-\Delta^2) + [x^4+2x^2(z^2-\Delta^2)+(z^2+\Delta^2)^2]\ln[(x+\Delta)^2+z^2/(x-\Delta)^2+z^2]^{1/2}}{[(x-\Delta)^2+z^2][(x+\Delta)^2+z^2]}\right\}^2, \quad (5)$$

where x is the distance from the particle center to the middle between the two electrodes, z is the distance from the particle center to the electrodes surface, and $2\Delta = 100\ \mu$m is the electrodes distance. The distance x is measured by image acquisition using Motic software, and z is measured by using microscope fine control while focusing subsequently on electrode surface and then on the particle surface; z is the difference between the two indications on fine control scale. The dielectrophoretic force is then calculated by Eq. (2). Figure 4 shows the field gradient diagram for the area between the electrodes and for z values of elevation from the microscope slide surface up to 40 μm. In Eq. (5) the value taken for the voltage is the one where the particle escapes the trap. Then the dielectrophoretic force equals the optical one. A detailed theoretical approach of the method will be published elsewhere in due time. Once the particle escapes the trap it moves either towards the electrode when we have p-DEP, or away from the electrode when we have n-DEP.

The experimental procedure was repeated over 500 times for different cells or beads and for each different numerical aperture of the microscope objective that was used, by increasing the laser power. For the electrical properties of the polystyrene the following values were used: $\varepsilon_p = 2.5\varepsilon_0$, for the dielectric permittivity, where ε_0 is the dielectric permittivity of the vacuum space, and $\sigma_p = 0.24$ mS/m, for the electric conductivity. The case of the yeast cells is more complicated, as we have to deal with a biological particle that has a complex structure. Thus, we must consider different values for the electrical properties of the cell membrane and the cytoplasm and then to combine them, taking into account also the thickness of the membrane, to extract the proper value for the complex permittivity.[31] The expression for a particle with shell becomes

$$\varepsilon^* = \frac{(r/r-d)^3 + 2(\varepsilon_c^* - \varepsilon_{\mathrm{mb}}^*/\varepsilon_c^* + 2\varepsilon_{\mathrm{mb}}^*)}{(r/r-d)^3 + (\varepsilon_b^* - \varepsilon_{\mathrm{mb}}^*/\varepsilon_c^* + 2\varepsilon_{\mathrm{mb}}^*)}, \quad (6)$$

where r is the particle radius, d is the membrane thickness, ε_c^* is the complex permittivity of the interior part of the cell (cytoplasm), and $\varepsilon_{\mathrm{mb}}^*$ is the complex permittivity of the cell membrane.

A membrane thickness of 12 nm was considered, while for the values of the dielectric permittivity and the conductivity for the membrane and the cytoplasm, respectively, we have $\varepsilon_{\mathrm{mb}} = 11.3\varepsilon_0$, $\sigma_{\mathrm{mb}} = 10^{-3}$ mS/m, and $\varepsilon_c = 50\varepsilon_0$, $\sigma_c = 500$ mS/m. Finally, the respective values for the distilled water are $\varepsilon_{\mathrm{m}} = 80\varepsilon_0$ and $\sigma_{\mathrm{m}} = 6.15$ mS/m. The real part of the Clausius-Mossoti factor, which determines the kind of dielectrophoresis we have, for the case of the polystyrene beads is $\mathrm{Re}(f_{\mathrm{CM}}) = -0.47$, which means that we have n-DEP, while for the yeast cells the mean value for different cell radii is about $\mathrm{Re}(f_{\mathrm{CM}}) = 0.87$, which means that in that case we have p-DEP.

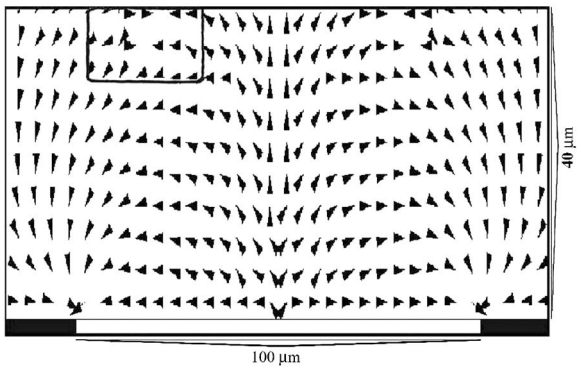

Fig. 4 Field gradient in the z plane for a voltage value of 5 V. For $z \sim 35\ \mu$m we can see the abnormality of the gradient, which creates the change in direction in the movement of the bead.

4 Results and Discussion

Trapping in three dimensions was achieved with both 40× and 100× objectives. Trapping was assured for a quite long distance on the z axis, up to 35 μm. The system, of the dielectrophoresis calibration experiment, detects a possible misalignment of optical tweezers. When the laser beam was not very well focused, the particle was trapped at a relatively high distance on the z axis. The field gradient shows a discontinuity for distances above $\sim 35\ \mu$m, as we can see in Fig. 4. In this case, the particle is trapped in such a high z value that when the electric field is applied it starts moving upward at higher z levels, as the axial trapping force is not sufficient to

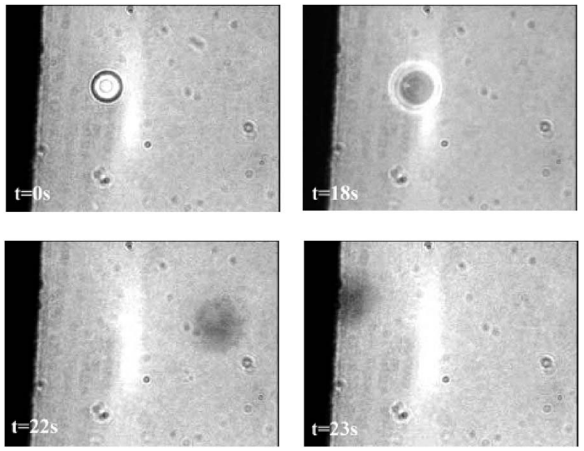

Fig. 5 Influence of the misalignment on the optical tweezers performance. The frames show a polystyrene bead changing its direction of travel under the action of the dielectrophoretic effect, as explained in detail in the text.

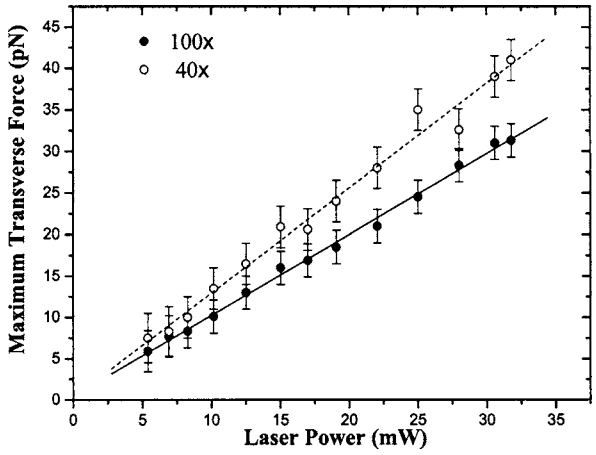

Fig. 6 Maximum transverse force determined through dielectrophoresis for 8-μm-diam polystyrene beads, using the 40× and the 100× objectives.

keep the particle well confined in the trap. In Fig. 5 we can see the movement of an 8-μm-diam polystyrene bead in a misaligned optical tweezers, when the voltage is increased. At $t=0$ s the bead experiences only the optical force. By increasing the voltage the bead is guided upward but remains trapped until $t=18$ s. Then the dielectrophoretic force slightly exceeds the optical one and the bead starts moving to the middle area of the electrodes. After a few seconds, we can see that the bead changes direction and moves toward the electrode's edge, while at the same time it keeps moving also upward (elevation being farther away from the focal point of the microscope objective). At this point, further elevation is due to the form of the field gradient in the middle between the two electrodes, where it has also a component in the z direction and thus the force pushes the particle in a different direction. Note that in the area of the abnormality of the field gradient, the dielectrophoretic force shows also a discontinuity. We can thus conclude that it is better to work in relatively small z distance (5 to 25 μm), where we can find an interval for the distance from the middle of the electrodes, where the dielectrophoretic force has a proper value.

For practical considerations, a dimensionless quality factor Q was introduced by Ashkin to give the measure for the efficiency of the laser trapping: $Q=Fc/Pn_1$, where F is the trapping force, P is the laser power, c is the light velocity, and n_1 is the refractive index of the medium.[34]

Figure 6 shows the transverse force against the laser power measured for polystyrene beads with radii of 8 μm, for the two microscope objectives used. The measured forces varied between ~6 and 40 pN when the laser power was increased from 5 to 32 mW. At this point, note that at low laser powers, the uncertainty in the estimation of the escape voltage is greater than at higher powers, so measurements at this region should be made very carefully. From the slopes of the linear approximation of the graphs the trapping efficiency was estimated. The efficiency measured for the 100× objective is $Q=0.22\pm0.03$, while that for the 40× objective is $Q=0.28\pm0.03$.

Figure 7 presents the respective graph for the case where the setup was tested by using yeast cells, and Table 1 shows the values for the trapping efficiency Q. Forces in the range from 0.5 to 38 pN were measured. In the case of the yeast cells, where a large number of measurements were performed, we had a larger variety of particle diameters in the range from 3.5 to 7.0 μm in each sample. However, as we had an uncertainty of 5% in measuring the diameter, the measured particles were studied in groups of those who had close diameters according to the estimated error and in the graphs we show only few representative values. The values that are mentioned in the table and the graphs are mean values for each group.

The efficiency values presented in this work are in the range of the Q values reported by other researchers.[34–36] Wright et al.[35] measured efficiency values, for different experimental setups, below 0.1, whereas Ashkin[34] reports trapping efficiencies up to 0.30. Fuhr et al.[36] report efficiencies of 0.077 for 4.9-μm-diam beads, 0.096 for 6.4 μm, 0.122 for 7.8 μm, and 0.174 for 12 μm, using a setup with two quadrupole-electrode systems and also taking advantage of the dielectrophoretic effect. Generally, we measured greater efficiency values than Fuhr, but the trapping setup and the dielectrophoretic field cage are totally different, so the comparison cannot be direct. However, a common notice could be that in both works the Q factor increases by increasing the particle diameter. From our results, it seems also that further increment of the particle diameter leads to a plateau. Fuhr also mentions that when a different objective was used, a possible misalignment led to nonlinear plots of the force versus power. By changing the objective in our setup, we did not noticed any important change in our measurements. Small deviations from linearity could be present in any case and that was obviously due to systematic errors.

In our results, we can also notice that trapping efficiencies obtained with the 40× objective tend to be generally higher than those obtained with the 100×. In the case of polystyrene beads this is obvious, while in the measurements performed with the yeast cells we can see (Fig. 8) that, apart from two or three cases, the general view that we get is the same. This result is in contradiction to what we would expect from the

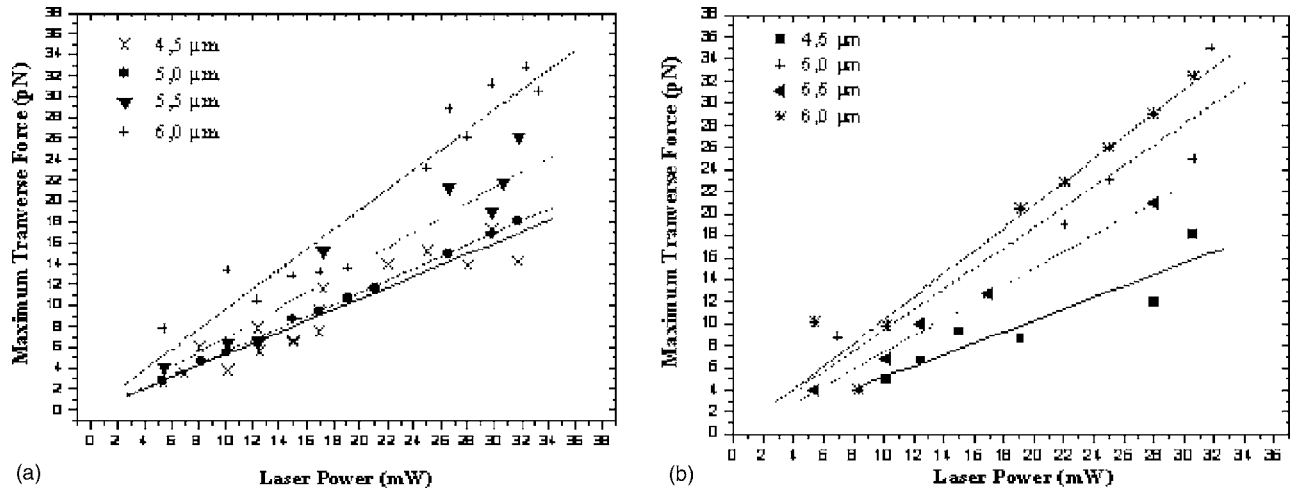

Fig. 7 Maximum transverse force determined through dielectrophoresis for yeast cells of several diameters, using the (a) 100× and (b) 40× objectives.

theory of optical tweezers. The use of a 100× immersion oil microscope objective is a crucial factor to obtain a very well focused and powerful trap, due to its high numerical aperture. However, it is not the first time that a similar observation is made. In the literature someone can find both views. Wright et al.,[35] reports higher efficiencies for higher numerical aperture objectives, but of the same magnification. The work of Malagnino et al.,[24] measuring the trapping efficiency of a tweezers system using a diode laser, and the viscous drag Stoke's forces as a calibration method, is closer to the work presented here, as they performed measurements with both 100× and 40× objectives of the same numerical aperture (NA) as that of the objectives that we used. This paper shows also that for particles with diameters greater than ~4 μm, the 40× objective was more efficient. The qualitative explanation that is given is based on the ray optics model. The trapping efficiency for particles larger than the beam waist is higher than for smaller particles because they take advantage of the whole beam. But, for the tightly focused beam, the smaller particles also experience the whole cross section of the more convergent rays. It is also mentioned that comparison with

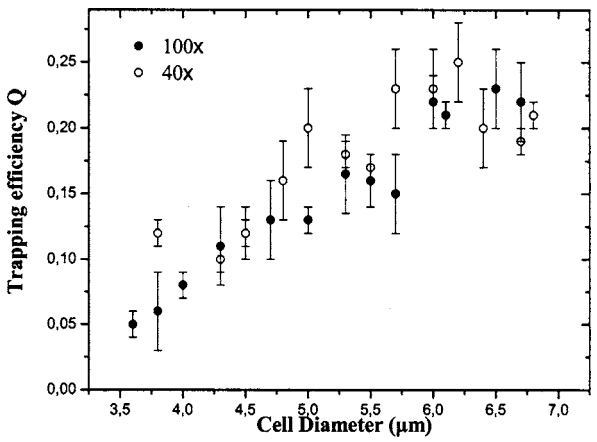

Fig. 8 Trapping efficiency versus cell diameter obtained with the 100× and 40× objectives.

numerical calculations of the axial and transverse forces performed by Harada and Asakura[37] for a wide range of particle size between 10^{-3} and 10 μm, considering a wavelength of 514 nm, showed a qualitative agreement in terms of orders of magnitude with this result. In addition, Malagnino et al. also noted that the Q factors for both NAs approached a plateau at large particle sizes (larger than 6 μm diameter). In any case, the Q values of that work, also, did not exceed the 0.1.

Thus, it is obvious that there is a wide spectrum of experimental data concerning force calibration of optical tweezers.[26,27,34–36,38,39] This fact can be attributed to several technical characteristics, which diversifies every experimental setup used. The most important characteristic is the optical quality of the microscope objective lens, as immersed objectives are sensitive to spherical aberrations.[35,40] Since the optical forces cannot be calculated exactly, it is very important to find easy ways to measure them directly and calculate the efficiency of laser trapping. The method that we describe here is an electrically controlled repetitive noncontact method. The whole concept is very simple and the setup is easy to construct. The two thin film parallel electrodes are easy to manufacture and handle, because they are in the form of a microscope slide. Their simple geometry makes the whole procedure a lot easier by simplifying the analytical and numerical calculations. More sophisticated geometries can lead to more complicated analyses, and more mathematical concessions.

Moreover, it was mentioned[36] that thermal gradients, induced by the laser focus inside the cell, change its permittivity and conductivity. The calculation of these gradients is also possible in similar setups and is very important, as they contribute in increasing the electric field gradient and they introduce anisotropies, enabling the creation of space charges.

Finally, in our setup, low voltages and a frequency far above the charge relaxation time were used, as already mentioned. Thus, hydrodynamic effects near the electrodes of high field strength are restricted and thermal streaming or electrophoretic effects become negligible.

Table 1 Trapping efficiency Q measured for the yeast cells.

Mean Cell Diameter (μm)	Q	
	100×	40×
3.6	0.05±0.01	—
3.8	0.06±0.03	0,12±0.01
4.0	0.08±0.01	—
4.3	0.11±0.03	0.10±0.01
4.5	0.12±0.01	0.12±0.02
4.7	0.13±0.03	—
4.8	—	0.16±0.03
5.0	0.13±0.01	0.20±0.03
5.3	0.17±0.03	0.18±0.01
5.5	0.16±0.02	0.17±0.01
5.7	0.15±0.03	0.23±0.03
6.0	0.22±0.02	0.23±0.03
6.1	0.21±0.01	—
6.2	—	0.25±0.03
6.4	—	0.20±0.03
6.5	0.23±0.03	—
6.7	0.22±0.03	0.19±0.01
6.8	—	0.21±0.01

5 Conclusions

An optical tweezers system based on an Ar^+ laser emitting at $\lambda=488$ nm was tested for two microscope objectives of different numerical aperture, namely, 0.65 (40× long-distance working) and 1.30 (100× immersion oil), by using 8.0-μm-diam polystyrene beads and 3.5 to 7.0-μm-diam yeast cells. Transverse optical forces were measured by taking advantage of the dielectrophoretic effect that appears when a dielectric particle is inserted in a nonuniform electric field. The dielectrophoretic force equals the optical one, which in this way can be easily calculated. The dielectrophoresis setup is simple in construction and easy to use, consisting of two thin film electrodes in the form of a microscope slide that simplifies analytical and numerical calculations of the electric field. To our knowledge this is the first time that so simple, but accurate, a dielectrophoretic chamber was used for optical tweezers calibration.

Forces in the range between ~6 and 40 pN were obtained for the 8.0-μm-diam polystyrene beads and in the range between 0.5 and 38 pN for the yeast cells, by increasing the laser power from 5 to 32 mW. The measured trapping efficiencies are generally in the same range reported by other researchers.[27,34–36] We have measured Q factors from 0.05 to 0.28, with the higher efficiencies achieved for the larger diameter particles. Comparing the trapping by two different NA lenses, we have noticed that, in the used diameter range, the 40× objective generally was found more efficient. Finally, by increasing the particle diameter the Q values showed a tendency to reach a plateau for both microscope objectives used.

Acknowledgments

This research effort is financially supported by the Heraclitus Project: Grants for basic research, cofunded by the European Social Fund (75%) and National Resources (25%). One of the authors (D. Pietreanu) is indebted to the Romanian-Greek bilateral cooperation project for financial assistance. Thanks are also due to Dr. D. Goustouridis from the Institute of Microelectronics of NCSR "Demokritos" for the construction of the dielectrophoretic electrodes setup.

References

1. A. Ashkin, J. M. Dziedzic, J. E. Bjorkholm, and S. Chu, "Observation of a single-beam gradient trap for dielectric particles," *Opt. Lett.* **11**, 288–290 (1986).
2. A. Ashkin, J. M. Dziedzic, and T. Yamane, "Optical trapping and manipulation of single cells using infrared laser beams," *Nature (London)* **330**, 769–771 (1987).
3. A. Ashkin, K. Schultze, J. M. Dziedzic, U. Euteneuer, and M. Schliwa, "Force generation of organelle transport measured in vivo by an infrared laser trap," *Nature (London)* **348**, 346–348 (1990).
4. S. C. Kuo and M. P. Sheetz, "Force of single kinesin molecules measured with optical tweezers," *Science* **260**, 232–234 (1993).
5. S. Block, L. S. B. Goldstein, and B. J. Schnapp, "Using optical tweezers to investigate kinesin-based motility in vitro," *J. Cell Biol.* **109**, 81a (1989).
6. A. Ashkin and J. M. Dziedzic, "Optical trapping and manipulation of viruses and bacteria," *Science* **235**, 1517–1520 (1987).
7. D. N. Rowell, "The double helix gets trapped," *Biophotonics Int.* **9**, 48–51 (2002).
8. T. Perkins, D. E. Smith, and S. Chu, "Direct observation of tube-like motion of a single polymer chain," *Science* **264**, 819–822 (1994).
9. K. O. Greulich, *Micromanipulation by Light in Biology and Medicine*, Birkhauser Verlag, Basel, Boston, Berlin (1999).
10. M. Dao, C. T. Lim, and S. Suresh, "Mechanics of the human red blood cell deformed by optical tweezers," *J. Mech. Phys. Solids* **51**, 2259–2280 (2003).
11. S. C. Grover, R. C. Gauthier, and A. G. Skirtach, "Analysis of the behavior of erythrocytes in an optical trapping system," *Opt. Express* **7**, 533–539 (2000).
12. C. T. Lim, M. Dao, S. Suresh, C. H. Sow, and K. T. Chew, "Large deformation of living cells using laser traps," *Acta Mater.* **52**, 1837–1845 (2004).
13. T. N. Buican, M. J. Smith, H. A. Crissman, G. C. Salzman, C. C. Stewart, and J. C. Martin, "Automated single-cell manipulation an sorting by light trapping," *Appl. Opt.* **26**, 5311–5316 (1987).
14. R. Steubing, S. Cheng, W. H. Wright, Y. Numajiri, and M. W. Berns, "Laser-induced cell fusion in combination with optical tweezers: the laser-cell fusion trap," *Cytometry* **12**, 505–510 (1991).
15. K. Svoboda and S. M. Block, "Biological applications of optical forces," *Annu. Rev. Biophys. Biomol. Struct.* **23**, 247–285 (1994).
16. M. W. Berns, W. H. Wright, B. J. Tromberg, G. A. Profeta, J. J. Andrews, and R. J. Walter, "Use of a laser-induced optical force trap to study chromosome movement on the mitotic spindle," *Proc. Natl. Acad. Sci. U.S.A.* **86**, 4539–4543 (1989).
17. H. Liang, W. H. Wright, S. Cheng, W. He, and M. W. Berns, "Micromanipulation of chromosomes in PTK2 cells using laser microsurgery (optical scalpel) in combination with laser-induced optical force (optical tweezers)," *Exp. Cell Res.* **204**, 110–120 (1993).
18. A. Erlicher, T. Betz, B. Stuhrmann, D. Koch, M. G. Raisen, and J. Käs, "Guiding neuronal growth with light," *Proc. Natl. Acad. Sci. U.S.A.* **99**, 16024–16028 (2002).
19. D. J. Odde and M. J. Renn, "Laser-guided direct writing for applica-

tions in biotechnology," *Nanotechnology* **17**, 385–389 (1999).
20. J. Xu, S. A. Grant, and R. L. Pastel, "Laser-guided direct writing: a novel method to deposit biomolecules for biosensor arrays," *IEEE Trans. Biomed. Eng.* **50**, 126–128 (2000).
21. A. Buosciolo, "New calibration method for position detector for simultaneous measurements of force constants and local viscosity in optical tweezers," *Opt. Commun.* **230**, 357–368 (2004).
22. E. Fällman, S. Schedin, J. Jass, M. Andersson, B. E. Uhlin, and O. Axner, "Optical tweezers based force measurement system for quantitating binding interactions: system design and application for the study of bacterial adhesion," *Biosens. Bioelectron.* **19**, 1429–1437 (2004).
23. M. C. Williams, "Optical tweezers: measuring piconewton forces," in *Biophys. Textbook Online* (2002).
24. N. Malagnino, G. Pesce, A. Sasso, and E. Arimondo, "Measurements of trapping efficiency and stiffness in optical tweezers," *Opt. Commun.* **214**, 15–24 (2002).
25. H. Chun-Cheng, C. C. Huang, C.-F. Wang, D. S. Mehta, and A. Chiou, "Optical tweezers as sub-piconewton force transducers," *Opt. Commun.* **195**, 41–48 (2001).
26. G. Martinot-Lagarde, B. Pouligny, M. I. Angelova, G. Grhean, and G. Gouesbet, "Trapping and levitation of a dielectric sphere with off-centred Gaussian beams: II. GLMT analysis," *J. Opt. A, Pure Appl. Opt.* **34**, 571–585 (1995).
27. J. P. Barton, D. R. Alexander, and S. A. Schaub, "Theoretical determination of net radiation force and torque for a spherical particle illuminated by a focused laser beam," *J. Appl. Phys.* **66**, 4594–4602 (1989).
28. W. H. Wright, G. J. Sonek, and M. W. Berns, "Radiation trapping forces on microspheres with optical tweezers," *Appl. Phys. Lett.* **63**, 715–717 (1993).
29. H. A. Pohl, "Some effects of nonuniform fields on dielectrics," *J. Appl. Phys.* **29**, 1182–1188 (1958).
30. H. A. Pohl, *Dielectrophoresis*, Cambridge University Press, Cambridge (1978).
31. B. T. Jones, "Basic theory of dielectrophoresis and electrorotation," *IEEE EMBS Magaz* **22**, 33–42 (2003).
32. D. Pietreanu, A. Mitrut, and M. Radu, "Optical tweezers force calibration using electrophoresis," in *Proc. Int. IUPAB School on Noninvasive Biophysical Methods in Medicine and Biology*, Abstract Book, p. 35 Predeal, Romania (2003).
33. D. Pietreanu, E. Papagiakoumou, M. Radu, T. Savopol, M. Makropoulou, A. Serafetinides, and E. Kovacs, "Optical tweezer and dielectrophoresis in studying the cell dielectric properties," *Proc. 49th Annual Meeting of Biophysical Society*, Abstracts Addendum pos-L172, p. 27, Long Beach, CA (2005).
34. A. Ashkin, "Forces of a single-beam gradient laser trap on a dielectric sphere in the ray optics regime," *Biophys. J.* **61**, 569–582 (1992).
35. W. H. Wright, G. J. Sonek, and M. W. Berns, "Parametric study of the force on a microsphere held by optical tweezers," *Appl. Opt.* **33**, 1735–1748 (1994).
36. G. Fuhr, T. Schnelle, T. Müller, H. Hitzler, S. Monajembashi, and K.-O. Greulich, "Force measurements of optical tweezers in electro-optical cages," *Appl. Phys. A* **67**, 385–390 (1998).
37. Y. Harada and T. Asakura, "Radiation forces on a dielectric sphere in the Rayleigh scattering regime," *Opt. Commun.* **124**, 529–541 (1996).
38. S. Sato, M. Ohyumi, H. Shibata, H. Hinaba, and Y. Ogawa, "Optical trapping of small particles using a 1.3-μm compact InGaAsP diode laser," *Opt. Lett.* **16**, 282–284 (1991).
39. C. d'Helon, E. W. Dearden, H. Rubinsztein-Dunlop, and N. R. Heckenberg, "Measured of the optical force and trapping range of a single beam gradient optical trap for micron-sized latex spheres," *J. Mod. Opt.* **41**, 595–601 (1994).
40. W. Singer, S. Bernet, N. Hecker, and M. Ritsch-Marte, "Three-dimensional force calibration of optical tweezers," *J. Mod. Opt.* **47**, 2921–2931 (2000).